Title

Increased expression of ApoE and protection from amyloid-beta toxicity in transmitochondrial cybrids with haplogroup K mtDNA.

Authors

Coskun, Pinar
Cáceres-Del-Carpio, Javier
Udar, Nitin
et al.

Publication Date

2016-09-01

DOI

10.1016/j.nbd.2016.04.005

Peer reviewed

HHS Public Access

Author manuscript

Neurobiol Dis. Author manuscript; available in PMC 2018 April 27.

Published in final edited form as:

Neurobiol Dis. 2016 September ; 93: 64–77. doi:10.1016/j.nbd.2016.04.005.

Increased expression of ApoE and protection from amyloid-beta toxicity in transmitochondrial cybrids with haplogroup K mtDNA

Kunal Thaker[a], **Marilyn Chwa**[a], **Shari R. Atilano**[a], **Pinar Coskun**[b], **Javier Cáceres-del-Carpio**[a], **Nitin Udar**[a], **David S. Boyer**[c], **S. Michal Jazwinski**[d], **Michael V. Miceli**[d], **Anthony B. Nesburn**[a,e], **Baruch D. Kuppermann**[a], and **M. Cristina Kenney**[a,f,*]

[a]Gavin Herbert Eye Institute, University of California Irvine, Irvine, CA, United States

[b]Department of Neurobiology and Behavior, University of California Irvine, Irvine, CA, United States

[c]Retina-Vitreous Associates Medical Group, Beverly Hills, CA, United States

[d]Tulane Center for Aging and Department of Medicine, Tulane University, New Orleans, LA, United States

[e]Cedars-Sinai Medical Center, Los Angeles, CA, United States

[f]Department of Pathology and Laboratory Medicine, University of California Irvine, Irvine, CA, United States

Abstract

Mitochondrial (mt) DNA haplogroups, defined by specific single nucleotide polymorphism (SNP) patterns, represent populations of diverse geographic origins and have been associated with increased risk or protection of many diseases. The H haplogroup is the most common European haplogroup while the K haplogroup is highly associated with the Ashkenazi Jewish population. Transmitochondrial cybrids (cell lines with identical nuclei, but mtDNA from either H ($n = 8$) or K ($n = 8$) subjects) were analyzed by the Seahorse flux analyzer, quantitative polymerase chain reaction (Q-PCR) and immunohistochemistry (IHC). Cybrids were treated with amyloid-β peptides and cell viabilities were measured. Other cybrids were demethylated with 5-aza-2′-deoxycytidine (5-aza-dC) and expression levels for *APOE* and *NFkB2* were measured. Results show K cybrids have (a) significantly lower mtDNA copy numbers, (b) higher expression levels for MT-DNA encoded genes critical for oxidative phosphorylation, (c) lower Spare Respiratory Capacity, (d) increased expression of inhibitors of the complement pathway and important inflammasome-related genes; and (e) significantly higher levels of *APOE* transcription that were independent of methylation status. After exposure to amyloid-$\beta_{1–42}$ peptides (active form), H haplogroup cybrids demonstrated decreased cell viability compared to those treated with amyloid-$\beta_{42–1}$ (inactive form) ($p < 0.0001$), while this was not observed in the K cybrids ($p = 0.2$). K cybrids had significantly higher total global methylation levels and differences in expression levels

*Corresponding author at: Gavin Herbert Eye Institute, Ophthalmology Research Laboratory, University of California Irvine, Hewitt Hall, Room 2028, 843 Health Science Road, Irvine, CA 92697, United States. mkenney@uci.edu (M.C. Kenney).

Conflict of interest statement

The authors have no conflict of interest to report.

for two acetylation genes and four methylation genes. Demethylation with 5-aza-dC altered expression levels for *NFkB2*, while *APOE* transcription patterns were unchanged. Our findings support the hypothesis that mtDNA-nuclear retrograde signaling may mediate expression levels of APOE, a key factor in many age-related diseases. Future studies will focus on identification of the mitochondrial-nuclear retrograde signaling mechanism(s) contributing to these mtDNA-mediated differences.

Graphical abstract

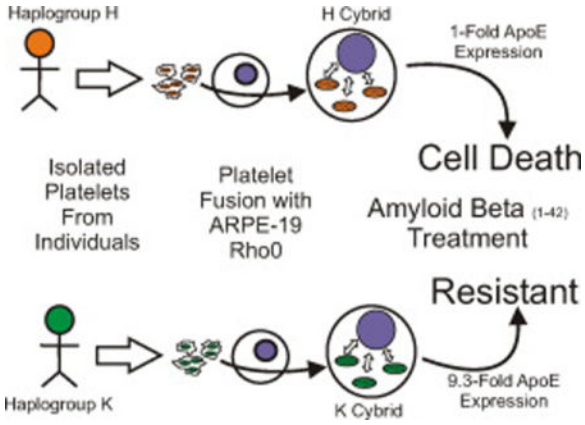

Keywords

Mitochondrial DNA; Haplogroup; Cybrids; APOE; Complement inhibitors; Inflammasome; Epigenetics; Amyloid-$\beta_{1–42}$

1. Introduction

Mitochondria (mt) are unique organelles with circular, double-stranded DNA containing 16,569 nucleotide pairs. The coding region of mtDNA encodes for 37 genes, including 13 protein subunits essential for oxidative phosphorylation (OXPHOS), 2 ribosomal RNAs and 22 transfer RNAs. (Wallace, 1992, 1994; McFarland and Turnbull, 2009) The non-coding region of 1121 nucleotides, known as the MT-Dloop, is critical for mtDNA replication and transcription. Most recently, it has been reported that biologically active mitochondrial-derived peptides (MDPs) are encoded from the *16s* and *12s* rRNA of the mtDNA. (Lee et al., 2015; Yen et al., 2013) Geographic origins of populations can be classified into haplogroups based upon the patterns of accumulated single nucleotide polymorphisms (SNPs) with the mtDNA.

Studies show that mtDNA haplogroups can confer either increased risk or protection for many human diseases, including Alzheimer's disease (AD) and age-related macular degeneration (AMD). (Wallace et al., 2007; Czarnecka and Bartnik, 2011; Ridge et al., 2012; Strauss et al., 2013; De Luca et al., 2012; Fernandez-Caggiano et al., 2013; Canter et al., 2006; Fernandez-Caggiano et al., 2012; Fesahat et al., 2007; Bi et al., 2015; Jones et al., 2007; Canter et al., 2008; Udar et al., 2009; SanGiovanni et al., 2009; Mueller et al., 2012a; Kenney et al., 2013a) Both Alzheimer's disease and AMD are associated with inflammation,

oxidative stress, specific ApoE allele profiles and amyloid-β deposits, along with risk factors including smoking, obesity, elevated cholesterol, hypertension and aging. (Kaarniranta et al., 2011; Zhao et al., 2015; Hyttinen et al., 2014) In these diseases, mitochondrial dysfunction, retrograde signaling, and epigenetic abnormalities altering nuclear gene expression also contribute to their pathogenesis. (Salminen et al., 2015; Hjelmeland, 2011; Guha and Avadhani, 2013; Whelan and Zuckerbraun, 2013) Therefore, intense interest has developed to understand the underlying mechanisms of these intricate mitochondrial-nuclear interactions.

A major hurdle in identifying the effects of mtDNA upon cellular homeostasis is the variability of nuclear genes from one individual to another. This problem can be addressed by using the transmitochondrial cybrid models, which are cell lines with identical nuclei, but the mtDNA from different subjects. Using the cybrid model, it has been demonstrated that different mtDNA haplogroups mediate cellular bioenergetics, the levels of methylation, rates of growth, and transcription of inflammatory, complement and signaling pathway genes. (Bellizzi et al., 2009; Gomez-Duran et al., 2010; Chen et al., 2012; Pacheu-Grau et al., 2013; Kenney et al., 2013b, 2014a, 2014b; Malik et al., 2014) In addition, cybrids with different mtDNA haplogroups have different responses to hydrogen peroxide or ultraviolet radiation. (Malik et al., 2014; Mueller et al., 2012b; Lin et al., 2012) The conplastic mouse model, which crosses the mtDNA from one strain of mouse into a different background, has illustrated altered mitochondrial-nuclear interactions and increased susceptibility to cardiovascular disease. (Fetterman et al., 2013) These studies support the hypothesis that an individual's mtDNA background contributes to baseline cellular homeostasis, making the cells differentially susceptible to identical stressors and contributing to differential disease susceptibility.

The UK cluster, comprised of both the U and K haplogroups, is defined by the A12308G SNP. The group diverges with the G9055A that defines the K haplogroup. The K mtDNA haplogroup (also known as Uk) has a 1–6% worldwide distribution (www.MitoMap.org). Approximately 10% of the ancestral Europeans fall within the K haplogroups. One group highly associated with the K haplogroup is the Ashkenazi Jewish population, which is defined as K1a1b1a, K2a2a and K1a9 subsets. (Behar et al., 2004) Within the Ashkenazi Jewish population, approximately 32% can be classified in the K haplogroup, a high percentage that has occurred due to a genetic bottleneck. (Behar et al., 2004) The H haplogroups are the most common European mtDNA haplogroup (www.mitomap.com). Those individuals of maternal African-origin possess the L haplogroup, which is the oldest and most diversified haplogroup. The diverse racial/ethnic populations have different risks for specific diseases. For example, African-Americans are susceptible to developing type 2 diabetes, obesity and prostate cancer. (Hatzfeld et al., 2012; Mensah et al., 2005; Kurian and Cardarelli, 2007) The Ashkenazi Jews are prone to having high levels of cholesterol and lipid along with other cardiovascular diseases at young ages. (Seftel et al., 1989; Jenkins et al., 1980) Scientifically, when studying the relationship between genetics and specific diseases, it is helpful to study well-defined, homogeneous populations so genetic changes can more easily be identified. (Guha et al., 2012) As a successful example of this approach, it was the examination of Ashkenazi Jews females that led to the identity of *BRCA1* and

BRCA2 genes being associated with breast and ovarian cancers. (Lancaster et al., 1997; Berchuck et al., 1998).

The Ashkenazi Jewish population is an excellent model to study age-related diseases because the number of founders is limited, there have been population bottlenecks (sharp reduction in population size due to environmental or sociological events) and the population tends to marry within their communities. (Atzmon et al., 2005) As populations age, then the likelihood for individuals to develop age-related diseases is increased. In the present study, we illustrate that although the human retinal pigment epithelial (RPE) cybrids all have identical nuclei, the cybrids with K haplogroup mtDNA have: (1) significantly increased expression of ApoE, a critical lipid transporter molecule associated with human diseases; (2) higher degree of protection from cytotoxic effects of amyloid-β_{1-42} (active form); (3) increased expression of inhibitors of the alternative complement pathways and important inflammasome-related genes; and (4) elevated bioenergetic respiratory profiles compared to the H cybrids. These findings suggest that an individual's mtDNA may, by as of yet unknown mechanism(s), contribute to lipid transport, cholesterol metabolism, complement activation and inflammation, factors critical for AMD, Alzheimer's disease and other age-related diseases.

2. Materials and methods

2.1. Cybrid cultures and culture conditions

Institutional review board approval was obtained from the University of California, Irvine (*#2003-3131*). Peripheral blood was collected in tubes containing sodium citrate and DNA was isolated with a DNA extraction kit (PUREGENE, Qiagen, Valencia, CA) and quantified using Nanodrop 1000 (Thermo Scientific, Wilmington, DE). Platelets were isolated by a series of centrifugation steps and final pellets were suspended in Tris buffer saline (TBS). ARPE-19 cells, are a human diploid cell line showing structural and functional properties similar to RPE cells in vivo, derived from human retinal epithelia (ATCC, Manassa, VA). (Dunn et al., 1998) The ARPE-19 cells were made Rho*0* (deficient in mtDNA) by serial passage in low dose ethidium bromide. (Miceli and Jazwinski, 2005) Cybrids were produced by polyethylene glycol fusion of platelets with Rho*0* ARPE-19 cells as described previously. (Kenney et al., 2013b) Cybrids were cultured until confluent in DMEM-F12 containing 10% dialyzed fetal bovine serum, 100 unit/mL penicillin and 100 μg/mL streptomycin, 2.5 μg/mL fungizone, 50 μg/mL gentamycin and 17.5 mM glucose. A total of 11 haplogroup H cybrids were produced and 10 haplogroup K cybrids were cultured to passage 5 for the experiments. The age, gender, and sub-haplogroup data are described in Table 1.

2.2. Inhibition of methylation in cybrid cultures

Experiments were performed to determine if inhibition of methylation sites in the K and H cybrids might affect the RNA expression for nuclear genes associated with age-related diseases. The H cybrids ($n = 3$) and K cybrids ($n = 3$), each from different individuals, were plated for 24 h, media were removed and replaced with the same media containing a final concentration of 250 nM 5-aza-2′-deoxycytidine (5-aza-dC, Sigma-Alrich, St. Louis, MO). The culture media containing 5-aza-dC was replaced every 24 h for a total incubation period

of 48 h. Cells were pelleted, RNA isolated and cDNA synthesized as described below. Q-PCR was performed with primers for *APOE* and *NF*κ-*B2*, run in triplicates and the experiments were repeated twice.

2.3. Amyloid-β treatment and cell viability measurement

The amyloid-$\beta_{1–42}$ (active form) and amyloid-$\beta_{42–1}$ (inactive form) peptides (Anaspec Protein, Fremont, CA) were reconstituted by diluting the initial stock in 1% NH_4OH to 2.77 mM according to manufacturer designation. The amyloid-β stock solutions were further diluted in 1× PBS to 100 μM, which were then stored in aliquots at −20 °C. At the time of the experiments, aliquots were thawed and diluted with culture media to 20 μM amyloid-$\beta_{1–42}$ prior to being added to the cells. The H ($n = 6$) and K ($n = 8$) cybrids were cultured 24 h in 96 well plates (5×10^4 cells/well). Cells were treated with fresh media plus 20 μM amyloid-$\beta_{1–42}$ and the untreated samples had their culture media changed. After an additional 24 h, 10 μL MTT (3-(4,5-Dimethylthiazol-2-yl)-2,5-diphenyltetrazolium bromide) reagent (Biotium, Hayward, CA) was added to each well for 2 h, and then the reaction was quenched by adding 100 μL DMSO. Plates were read immediately with an absorbance reader at 570 nm (MTT) and at 630 nm (background) (Biotek elx808 Absorbance Reader, Winooski, VT). Background was subtracted from the MTT values and values were normalized to the corresponding untreated value. For each sample, the treated cultures were run as sextuplets and the untreated samples were run as quadruplets.

2.4. Oxygen consumption rates and biogenetic profiles

The Seahorse XF24 flux analyzer (Seahorse Bioscience, Billerica, MA) allows for real-time bioenergetic measurements in individual wells of the oxygen consumption rates (OCR) representing the basal aerobic respiration of the cells, extracellular acidification rates (ECAR) representing glycolysis, basal respiration, ATP turnover, maximal respiration, spare respiratory capacity, proton leak and non-mitochondrial respiration (Fig. 1). Cybrids with haplogroups H ($n = 7$) and K ($n = 10$) were plated at 30,000 cells/well and cultured overnight at 37 °C under 5% CO_2. Samples were run in triplicate and experiments repeated twice. Plates were then washed and placed 1 h in a 37 °C incubator under air in 500 μL of unbuffered DMEM (Dulbecco's modified Eagle's medium, pH 7.4), supplemented with 17.5 mM Glucose (Sigma, St Louis, MO), 200 mM L-glutamine (Invitrogen-Molecular Probes, Carlsbad, CA) and 10 mM sodium pyruvate (Invitrogen-Molecular Probes). There was sequential injection into the wells of Oligomycin (1 μM final concentration, which blocks ATP synthase to assess respiration required for ATP turnover), FCCP (1 μM final concentration, a proton ionophore, which induces chemical uncoupling and maximal respiration), and Rotenone plus Antimycin A (1 μM final concentration of each, completely inhibits electron transport to measure non-mitochondrial respiration). Total protein was isolated with RIPA lysis buffer (Millipore, Billerica, MA) containing protease inhibitor (Sigma, St. Louis, MO) and phosphatase arrest (G-Biosciences, St. Louis, MO). Isolated protein was mixed with Qubit buffer and measured with Qubit 2.0 fluorometer (Invitrogen, Grand Island, NY). Data from each well was normalized by measuring total protein levels.

Using the XF Reader software from Seahorse Bioscience, the bioenergetic profiles for the H and K cybrids were analyzed. The OCR is determined by measuring the drop in O_2 partial

pressure over time followed by linear regression to find the slope. The ECAR is determined by measuring the change in pH levels over time followed by linear regression to find the slope of the line that represents ECAR. The percentage ATP Turnover Rate is calculated by the following formula: 100 − (ATP coupler response/basal respiration × 100). The percentage Spare Respiratory Capacity represents a bioenergetic value for cells needing high amounts of ATP in response to demands placed upon them. This is calculated by the formula: Electron transport chain (ETC) accelerator response/basal respiration × 100. The percentage Proton Leak equals the ATP coupler response-non-mitochondrial respiration. Data from these experiments were exported to GraphPad Prism 5 (GraphPad Software, La Jolla, CA, USA) where they were analyzed, normalized and graphed. Statistical significance was determined by performing two-tailed Student *t* tests and $p \leq 0.05$ was considered significant in all experiments.

2.5. Whole mtDNA genome sequencing

The sequencing method was a modified version used by Zaragoza.(Zaragoza et al., 2011) The PCR for whole mtDNA genome sequencing was performed in two parts with a high fidelity PCR system (FailSafe™ PCR System, EpiCentre Biotechnologies, Madison, WI). Part A was with primers hmtL569 [AACCAAACCCCAAAGACAC] and hmtH12111 [AAACCCGGTAATGATGTCGG], while Part B was with primers hmtL11727 [GCCCACGGGCTTACATC] and hmtH1405 [ATCCAC CTTCGACCCTTAAG] (Integrated DNA Technologies, Inc., Coralville, IA). PCR products were run on a 1% agarose gel and then a single step enzymatic elimination of the unincorporated primers and dNTPs was performed (ExoSAP-IT, Affymetrix, Santa Clara, CA). Samples were sent to ELIM BioPharm for sequencing with internal primers (ELIM Biopharm, Hayward, CA). Sequencing results were analyzed with DNA variant analysis software (Mutation Surveyor, SoftGenetics, State College, PA).

2.6. Isolation of RNA and amplification of cDNA

Cells from cybrid cultures (H cybrids, $n = 8$; K cybrids, $n = 9$) were pelleted and RNA isolated using the RNeasy Mini-Extraction kit (Qiagen).(Kenney et al., 2013b) Individual RNA samples (100 ng) were reverse transcribed into cDNA with the QuantiTect Reverse Transcription Kit (Qiagen) and used for Q-PCR analyses.

2.7. Gene expression arrays and statistical analyses

For gene expression array analyses, equal quantities of RNA isolated from H cybrids ($n = 3$ different individuals) and K cybrids ($N = 3$ different individuals) were combined (250 ng/μL per sample) into two different samples for analyses by the UCLA Clinical MicroArray Core Lab (Affymetrix Human U133 Plus 2.0 Array).(Kenney et al., 2013b) The INGENUITY Systems pathway software (Redwood City, CA) was used to analyze the gene expression results.

2.8. Quantitative PCR (Q-PCR) analyses

Q-PCR was performed using different primers (QuantiTect Primer Assay, Qiagen) for genes associated with the atherosclerosis signaling pathway (*APOE*, *APOC1*, *COLA1* and

MMP1); amyloid beta precursors (*APBB1IP*, *APBB2*, and *APBA1*); inflammation and inflammasome pathways (*IL-6*, *IL-33*, *IL-1*β, *IL-18*, *CASP1*, *TGFA* and *TGF*β*2*); complement pathway (*C3*, *CFH*, *CD59*, *CD55*/*DAF*, *CFHR4*, *CFP*, *C4B*, *C1S*, *C1QC*, *CFD*, and *CFI*); and signaling pathways (*THBS1*, *HSPG2*, *ITGB5*, *ITGB8*, *NF*κ*B*, *MAPK8* and *MAPK10*). Primers for *ApoB*, *ABCA4*, *NLRP3* and *NLRP14* were also used, but extremely low expressions for these genes were found (*data not shown*). Total RNA was isolated from individual pellets of cultured cells of haplogroup H cybrids ($n = 8$ different individuals) and K cybrids ($n = 9$ different individuals) as described above. Previous studies have shown that mtDNA can modulate the expression of various genes associated with epigenetic pathways. (Atilano et al., 2015) Therefore, in this study we also analyzed *HAT1*, *HDAC1*, *HDAC6*, *HDAC11*, *SIN3A*, *MAT2B*, *MBD2*, *MBD4*, *DNMT1*, *DNMT3A* and *DNMT3B*. Q-PCR was performed on individual samples using a QuantiFast SYBR Green PCR Kit (Qiagen) on a Bio-Rad iCycler iQ5 detection system. Primers were standardized with the *HPRT1*, *HMBS*, *ALASv1*, *TUBB* or *GUSB* housekeeping genes. The mtDNA copy numbers for the H and K cybrids were determined by Q-PCR using 18S to represent nuclear DNA (nDNA) and MT-ND2 to represent mtDNA (TaqMan, Life Technologies). All samples and analyses were performed in triplicate.

2.9. Histochemical staining

The ApoE protein was analyzed by staining the H cybrids ($n = 6$) and K cybrids ($n = 7$) with the polyclonal antibody apolipoprotein E (GeneTex, Irvine, CA). Briefly, cells were plated onto 4-well tissue culture slides (Millipore, Billerica, MA), incubated for 120 h, rinsed in 1× PBS and then fixed with 2% paraformaldehyde. Cells were rinsed three times in 1× PBS and were treated overnight with ApoE antibody (diluted 1:100 in Triton X-100 with 0.02% bovine serum albumin (BSA)). The secondary donkey anti-rabbit antibody (GeneTex, Irvine, CA) was incubated for one hour (1:250 in Triton X-100 with 0.02% BSA). Upon washing with 1× PBS (five minute each) solution, the nuclei were stained with DAPI dilactate by incubating for fifteen minutes (Invitrogen, Carlsbad, CA). Slides were then mounted with 50/50 glycerol/1× PBS for imaging. The ApoE staining was visualized with the Nikon Eclipse E600 (Nikon, Tokyo, Japan); images taken using the CoolSNAP fx (Photometrics, Tuscon, AZ).

2.10. Statistical analyses

Data were subjected to statistical analysis by ANOVA, GraphPad Prism (Version 5.0). Newman–Keuls multiple-comparison test was done to compare the data within each experiment. $P < 0.05$ was considered statistically significant. Error bars in the graphs represent SEM (standard error mean).

3. RESULTS

3.1. Oxygen consumption rates and biogenetic profiles

For the H cybrids and K cybrids, the OCR to ECAR ratios (8.1 ± 0.88 versus 6.5 ± 1.04, $p = 0.28$), percentage ATP turnover rates (48.4 ± 1.8 versus 43.6 ± 3.1, $p = 0.25$) and Non-mitochondrial Respiration levels (31.6 ± 1.8 versus 33.3 ± 3.2, $p = 0.7$) were similar to each other (Fig. 1a). The K cybrids had significantly lower Spare Respiratory Capacity compared

to the H cybrids (133.2 ± 4.8 versus 153.6 ± 5.3, $p = 0.01$), but had elevated levels of Proton Leak (23.6 ± 1.1 versus 18.6 ± 1.04, $p = 0.02$).

3.2. Levels of expression for mtDNA encoded respiration genes

The expression levels of the mtDNA encoded genes in respiratory Complexes I, III, IV, and V of the OXPHOS pathway were measured and the H cybrids values normalized to 1 (Fig. 1b). The K cybrids showed significantly higher gene expression levels of ten of the twelve mtDNA encoded genes compared to H cybrids: Complex I, mt-ND1 (2.1-fold, $p = 0.0011$), mt-ND4/ND4L (1.6-fold, $p = 0.0078$), mt-ND5 (3.0-fold, $p < 0.0001$); mt-ND6 (2.5-fold, $p < 0.0001$); Complex III, mt-CYB (2.2-fold, $p < 0.0002$); Complex IV, (mt-CO1 (3.4-fold, $p < 0.0001$), mt-CO2 (2.2-fold, $p < 0.0001$), mt-CO3 (2.1-fold, $p < 0.0001$); Complex V, mt-ATP6 (2.0-fold, $p = 0.0005$); and mt-ATP8 (2.3-fold, < 0.0001). Fig. 1c shows that the K cybrids had lower mtDNA copy numbers (nDNA:mtDNA ratio) compared to the H cybrids after being cultured for 1 day ($p < 0.0001$) and 7 days ($p < 0.0055$).

3.3. GeneChip arrays analyses

The cDNA from K cybrids and H cybrids were analyzed with the Human Genome U133 Plus 2.0 Array and Ingenuity Software Program. Results from the Atherosclerosis Signaling pathway showed differences in genes between the K cybrids versus H cybrids (Table 2). The APOE genes had a 6.19-fold higher (Probe Set ID 203381 and Public ID number N33009) and 4.12-fold higher expression (Probe Set ID 203382, Public ID number NM_000041). In addition, the K cybrids showed higher gene expression levels for MMP1 (4.74 fold, Probe Set ID 204475/Public ID number NM_002421) and APOC1 (2.89-fold, Probe Set ID 204416/Public ID number NM_001645) but lower levels for APOC1 (−4.9 fold, Probe Set ID 213553/Public ID number W78384). The COL1A1 gene variants were also expressed at lower levels in the K cybrids (−3.56 fold, −4.19 fold and −11.1 fold, Probe Set IDs 202,310, 202,311 and 1,556,499/Public ID number K01228, A1743621 and BE221212, respectively).

3.4. Differences of gene expression in H cybrids versus K cybrids

Q-PCR analyses on individual H ($n = 8$) and K ($n = 8$) cybrid samples were used to verify the GeneChip Array results (Table 3). The K cybrids had a 9.3-fold higher ApoE (NM_000041) expression level compared to the H cybrids ($p < 0.0001$). In contrast to the GeneChip results, the Q-PCR analyses showed that the APOC1, COL1A1 and MMP1 genes were similar to each other in the H and K cybrids.

Amyloid-β, inflammation and complement activation contribute to the pathological processes of both AMD and Alzheimer's disease. The genes related to the amyloid-β pathway (*APBB1IP*, *APBB2* and *APBA1*) were analyzed and expressed similar levels for the H and K cybrids. The K cybrids had significantly increased expression of *IL-1*β (4.1-fold, $p = 0.001$), *IL-18* (2.6-fold, $p = 0.0007$) and *CASP1* (2.5-fold, $p < 0.0001$) compared to the H cybrids. The K cybrids had significantly elevated expression of the *C3* gene (4.4-fold, $p < 0.0001$) and also genes related to inhibition of the complement system (*CFH*, 2.4-fold, $p = 0.001$; *CD59*, 2-fold, $p = 0.004$; *CFD*, 1.8-fold, $p = 0.009$ and *CFI*, 2.2-fold, $p = 0.025$) compared to the H cybrids. There was lower expression in K cybrids for *CFHR4*, a cofactor

of *CFH* (0.4-fold, $p = 0.01$). The transcription levels for the pro-inflammatory cytokines *IL-6* and *IL-33* were similar to each other in the H and K cybrids.

Specific integrin/binding genes associated with AMD and Alzheimer's pathology were also analyzed in the cybrids. The K cybrids showed lower levels of *THBS1*, an adhesive glycoprotein that mediates cell-to cell and cell-to-matrix interactions compared to the H cybrids (0.4-fold, $p = 0.0009$), but increased levels of *ITGB8* (1.5-fold, $p < 0.0001$) and *NFKβ2* (1.5-fold, $p = 0.005$) compared to the H cybrids. The *MAPK8* and *MAPK10* expression levels were similar in the H and K cybrids.

3.5. Immuno-histochemical staining for ApoE

The H cybrids and K cybrids were cultured on chamber slides and stained with a polyclonal antibody to ApoE protein (Fig. 2a). A representative H cybrid showed regular punctate staining pattern along cellular periphery, while the K cybrids showed larger, globular staining patterns. The cultures stained with secondary antibody alone showed no fluorescent staining. The levels of ApoE fluorescence were quantified in H ($n = 6$) and K ($n = 7$) cybrids (Fig. 2b). The intensity of ApoE staining was significantly higher in the K cybrids (1.14 ± 0.034) compared to the H cybrids (1.00 ± 0.036, $p = 0.007$).

3.6. Response of cybrids to amyloid-β treatment

ApoE levels have been correlated to the elimination rates of amyloid-β. The H and K cybrids were treated for 24 h with 20 μM amyloid-$\beta_{1–42}$ (active form) and the cell viabilities were measured (Fig. 3). Some cultures were treated with the amyloid-$\beta_{42–1}$ peptide (inactive form), which served as a control. The H cybrids showed a 31% ± 2% decrease in cell viability after exposure to amyloid-$\beta_{1–42}$ compared to untreated H cybrids ($p < 0.0001$). The cybrids K cybrids had a 16% ± 2% decrease in cell viability compared to untreated K controls ($p < 0.0001$). The cybrids treated with amyloid-$\beta_{42–1}$ peptide (inactive form) had a 10% ± 3% decrease in cell viability compared to the untreated controls ($p = 0.01$). The H cybrids treated with amyloid-$\beta_{1–42}$ (active form) showed significant decline in cell viability compared to H cybrids treated with the inactive form (amyloid-$\beta_{42–1}$ peptide) control samples (20% ± 4%, $p < 0.0001$). In contrast, the K cybrids treated with amyloid-$\beta_{1–42}$ (active form) were not significantly decreased when compared to K cybrids treated with inactive, control amyloid-$\beta_{42–1}$ peptide (6% ± 0.05, $p = 0.2$).

In summary, data from the GeneChip arrays, Q-PCR analyses and staining techniques showed that the even though all cybrids had the identical nuclear genome, cells with K haplogroup mtDNA showed increased expression of *APOE* expression. When amyloid-$\beta_{1–42}$ peptides were added to the cybrids cultures, the H cybrids depicted the greatest degree of damage, while the K cybrids were significantly more protected.

3.7. Altered expression levels of genes associated with epigenetic pathways

The K cybrids ($n = 6$) were compared to the H cybrids ($n = 6$) for their expression levels of eleven epigenetic genes measured by Q-PCR (Fig. 4a). The K cybrids had lower expression levels for *HAT1* (0.8-fold, $p = 0.04$), *SIN3A*, a transcriptional regulator protein which promotes deacetylation (0.7-fold, $p = 0.0006$); *MBD4*, which binds specifically to

methylated DNA (0.5-fold, $p < 0.0001$); *DNMT1*, which methylate CpG sites (0.6-fold, $p < 0.0001$); and *DNMT3B*, which methylates DNA de novo (0.6-fold, $p = 0.002$) compared to the H cybrids. The *DNMT3A* expression was significantly higher in the K cybrids compared to the H cybrids (1.4-fold, $p = 0.03$). The expression levels for, *HDAC1*, *HDAC6*, *HDAC11*, *MAT2B*, and *MBD2* genes were similar in the K and H cybrids.

3.8. Elevated levels of global DNA methylation in K cybrids versus H cybrids

Previous studies have shown that the J mtDNA haplogroups have a 3.1-fold higher level of methylation compared to the H cybrids. (Atilano et al., 2015) The H and K cybrids were grown under identical conditions for 48 h and total global methylation levels were measured. The 5-mC% mean values were 0.005 ± 0.001 for the H cybrids and 0.032 ± 0.009 for the K cybrids ($p = 0.13$), which represents a 6.2-fold higher level of total global methylation for the K cybrids (Fig. 4b).

3.9. Methylation inhibitor studies

Experiments were conducted to determine if methylation was involved with the elevated expression of *APOE*. The H and K cybrids were treated with 5-aza-dC, a known inhibitor of methylation, and then the expression levels of *APOE* and *NFκB2* were measured (Fig. 4c). In the K cybrids, the *APOE* transcription levels were significantly higher in both the untreated (2.3-fold, $p = 0.001$) and 5-aza-dC treated cultures (3.8-fold, $p < 0.0001$) compared to the H cybrids. In contrast, the *NFκB2* expression levels were altered after inhibition by 5-aza-dC. Prior to inhibition, the K cybrids had a 3-fold higher expression of *NFκB2* ($p = 0.004$) compared to the H cybrids, but after 5-aza-dC treatment there was not a significant difference (1.5-fold, $p = 0.07$). These data indicate that the mtDNA variants can influence transcription levels of methylation and acetylation genes, the total global methylation levels and also the expression levels of *NFκB2*, a major signaling molecule. However, the differences in *APOE* expression in the H and K cybrids are not due to methylation status of the cells.

3.10. mtDNA haplogroup patterns of the H and K cybrids

The entire mtDNA from each of the cybrids (H cybrids, $n = 7$ and K cybrids, $n = 9$) were sequenced and compared to the Cambridge Reference Sequence (Fig. 5). The flow chart shows the assigned haplogroup subset, which is based upon the accumulation of specific SNPs. Each box describes the SNPs defining the subsets, some of which are non-synonymous and the amino acid changes are listed. The specific haplogroups of the H (Fig. 5a) or K (Fig. 5b) subjects used in this study have bolded boxes. None of the SNPs found in either the H or K cybrids were associated with diseases when compared to the www.MitoMap. org. *Reported Mitochondria DNA Base Substitution in Diseases* section or the *Coding and Control Region Point Mutations* section. Our sequencing data supports our theory that the different accumulations of SNPs representing the K haplogroups versus the H haplogroups results in amino acid changes within the mtDNA genes.

4. Discussion

In this report, we demonstrate that cybrids containing the K haplogroup mtDNA express higher levels of *APOE* than H haplogroup cybrids, even though all cybrids have identical nuclear genomes and tissue culture conditions. Our data support the hypothesis that mtDNA-nuclear retrograde signaling mediates transcription levels of *APOE,* a common element in many age-related diseases, including Alzheimer's disease, AMD, cardiovascular disorders, cancers and diabetes (Fig. 6).

A key pathologic feature is the accumulation of amyloid-β peptides within the Alzheimer's brains (Dorey et al., 2014; Murrell et al., 2006) and retinal drusen of AMD patients (Kaarniranta et al., 2011; Ratnayaka et al., 2015). Verghese and co-workers (2013) have reported that ApoE protein can affect the metabolism of soluble amyloid-β via interactions with cellular receptors/transporters and membrane surfaces. (Verghese et al., 2013) In our study, we exposed H and K cybrids to amyloid-$\beta_{1–42}$ peptide (active form) and amyloid-$\beta_{42–1}$ peptide (inactive form) and measured cell viability. The H cybrids treated with amyloid-$\beta_{1–42}$ demonstrated a 31% decrease in cell viability ($p < 0.0001$) when compared to untreated cultures. By comparison, the K cybrids treated with amyloid-$\beta_{1–42}$ declined only 16% in cell viability ($p < 0.0001$). When cybrids were treated with the amyloid-$\beta_{42–1}$ peptide (inactive form), there was a 10% decrease in cell viability ($p = 0.01$), indicating that the presence of the inactive peptide alone promoted a small amount of toxicity. The cell viability for the amyloid-$\beta_{1–42}$ treated K cybrids was not significantly different from the cybrids treated with the inactive amyloid-$\beta_{42–1}$ peptide (84% versus 90%, $p = 0.23$). We can speculate that in the K cybrids, the significantly higher levels of ApoE may play a role in higher clearance of amyloid-β and thereby, promoted cellular protection. However, further experiments are needed to elucidate the mechanism(s) for these specific interactions.

It has been shown that ApoE protein isoforms have direct interactions with amyloid-β to enhance the clearance.(Verghese et al., 2013) In neural cells, the ApoE ε2 allele suppresses the amyloid-β inflammatory response while the ApoE ε4 allele promotes it.(Dorey et al., 2014) The ApoE ε4 allele, which confers higher risk for lobar cerebral micro-bleeds, (Romero et al., 2014) has also been used to determine the initial responses and subsequent outcomes for acute brain injury (Graham et al., 1999) and is linked to elevated low-density lipoprotein (LDL) cholesterol levels. In a recent study, subjects with the K haplogroup are protected against traumatic brain injury and strong interactions were found between the ApoE ε4 allele and K haplogroup. (Bulstrode et al., 2014) However, if patients lacked the ApoE ε4 allele, then the K haplogroup did not have any impact on the outcome against the traumatic brain injury. (Bulstrode et al., 2014) In Alzheimer's patients, the K haplogroup neutralizes harmful effects of the ApoE ε4 allele. (Carrieri et al., 2001) In our cybrid model, the host RPE cells have ApoE ε3, ε3 alleles, and therefore, both the H and K cybrids have the same ApoE ε3, ε3 alleles. Therefore, the increased *APOE* gene expression in the K cybrids is likely due to retrograde signaling of mtDNA variants influencing the mitochondrial-nuclear interactions, which is a new concept for the production of *APOE* and promotes the importance of evaluation of the mtDNA variants for subjects with ApoE-related diseases.

It should be noted that ApoE is associated with AMD for European populations, but it is not a susceptibility factor in the Chinese population. (Sun et al., 2011) One can speculate that having the ApoE ε4 allele on the K haplogroup background might confer different risks compared to having the same allele on the Chinese haplogroup background, since each ethnic/racial population has every different haplogroup-defining SNPs. This is an especially attractive theory since reports show that specific mtDNA haplogroup backgrounds can increase the severity of a disease when coupled with either mitochondrial or nuclear mutations. For example, in patients with Leber Hereditary Optic Neuropathy (LHON), there is higher risk for vision failure when the mt3460G > A mutation is present on the K haplogroup background and there is a significantly lower risk if the mt11778G > A is on the H haplogroup background. (Hudson et al., 2007) It is also true for subjects with the nuclear mutation in the adenine nucleotide transloactor-1 (*ANT1*) gene, which causes cardiomyopathy. If the patients have the U haplogroup background, they have a more rapid and severe course of the disease compared to subjects with the H haplogroup. (Strauss et al., 2013).

Studies have demonstrated the mtDNA can mediate the epigenetic status of cells. (Atilano et al., 2015; Bellizzi et al., 2012; Smiraglia et al., 2008; Naviaux, 2008; Wallace and Fan, 2010; Bellizzi et al., 2013). In the present study, we examined the methylation- and acetylation-related genes in the K versus H cybrids. These differences in methylation status may help explain the personalized responses of individuals or populations to diseases and drug responses. The K cybrids had altered expression levels for two acetylation genes (*HAT1* and *SIN3A*) and four methylation-related genes (*MBD4*, *DNMT1*, *DNMT3A* and *DNMT3B*) compared to the H cybrids. Measurement of total global DNA methylation depicted the K cybrids had significantly higher levels compared to the H cybrids (6.2-fold, $p = 0.013$). Other studies have also shown that mtDNA can influence the methylation status of cells in vitro and it is highly likely to also affect cells in vivo. For example, increased total global DNA methylation levels have been reported in the J cybrids cells (3.1-fold, $p = 0.02$) (Atilano et al., 2015) and the osteosarcoma cybrids with J haplogroup mtDNA. (Bellizzi et al., 2012) These differences in epigenetic gene expression levels and methylation status can influence the retinal cell's mitochondrial homeostasis. (Smiraglia et al., 2008; Naviaux, 2008; Wallace and Fan, 2010) In addition, methylation levels have been associated with disease outcomes in atherosclerosis, late onset Alzheimer's disease, AMD, cancers and other age-related diseases. (Wallace and Fan, 2010; Grimaldi et al., 2015; Di Francesco et al., 2015; Pogribny and Rusyn, 2013).

In an effort to determine if the altered expression levels of *APOE* were mediated by methylation status, the cybrids were treated with 5-aza-dC, a methylation inhibitor, and downstream nuclear genes were evaluated. Our results suggest that although the mtDNA haplogroup within cells can significantly influence epigenetic profiles (expression levels of methylation and acetylation-related genes and influence total global methylation status) the expression levels of the APOE was not modulated via the methylation process. The *APOE* gene expression levels in the K cybrids before and after 5-aza-dC treatment were significantly higher that the H cybrids, indicating that the regulation for *APOE* was not related to the methylation status. In contrast, the NFκB2 levels in the untreated K cybrids were significantly higher (3-fold, $p = 0.004$) compared to the untreated H cybrids but after

demethylation, the expression levels were similar to each other (1.5-fold, $p = 0.07$). This suggests that methylation status plays a role in expression of NFκ*B2*, similar to what has been reported previously with the H and J cybrids. (Atilano et al., 2015).

4.1. Bioenergetics of K haplogroup cybrids

One potential mechanism of retrograde signaling is via the respiratory metabolism and ATP homeostasis. (Zhang et al., 2013) The K cybrid cultures had significantly higher expression levels of ten of twelve MT-RNA genes (range 1.62-fold to 3.43-fold), which are critical in the electron transport chain (ETC) and oxidative phosphorylation (OXPHOS). In a previous study, cybrids with L haplogroup mtDNA (African-maternal lineage) had significantly increased expression of nine of twelve genes (range 1.57-fold to 2.11-fold) and lower expression of one mtDNA encoded gene (0.16-fold, $p = 0.0048$) compared to the H cybrids. (Kenney et al., 2014a) In stark contrast to both the L and K cybrids, the J cybrids, cultured under identical conditions and with identical nuclei, preferentially use glycolysis and had significantly decreased expression of seven of out of the twelve measured mtDNA encoded genes (range 0.43-fold to 0.68-fold). (Kenney et al., 2013b) These findings are consistent with those reported in osteosarcoma cybrids (Gomez-Duran et al., 2010; Arning et al., 2010) and demonstrate that the mtDNA profile representing different haplogroups can influence the mode and efficiency of energy production, in spite cells having the same nuclear genome.

Prior investigations show that mtDNA variants in different ethnic/racial populations can mediate different responses in the complement/inflammatory systems. In our previous studies, we reported either unchanged or lower transcription levels for complement inhibitor genes (*CFH*, *CD55*, *CD59*) in the African-maternally inherited L cybrids compared to the common European H cybrids. (Kenney et al., 2014a) In the present study, we analyzed the complement genes and found the K cybrids had significantly elevated expression of complement inhibitors genes (*CFH*, 2.4-fold, $p = 0.001$; *CD59*, 2-fold, $p = 0.004$; and *CFI*, 2.2-fold, $p = 0.025$), which would block activation of complement pathways. Compared to the H cybrids, the K cybrids also showed significantly elevated expression of important inflammasome-related genes (*IL-1*β, 4.1-fold, $p = 0.001$, *IL-18*, 2.6-fold, $p = 0.0007$ and *CASP1*, 2.5-fold, $p < 0.0001$). These findings suggest that cells with the K mtDNA might favor the inflammasome pathways rather than activation of complement pathways. If this would hold true in K haplogroup populations, then these groups would have a more robust inflammasome response and perhaps less complement associated diseases, thereby contributing to the difference in disease susceptibilities. Future studies should strive to identify mtDNA-nuclear retrograde signaling that acts as a “master switch” to influence the gene expression levels of critical gene expression pathways common to many age-related diseases.

5. Conclusion

Although K and H cybrids have identical nuclear genomes, the variants within the mtDNA result in differences in transcription levels for MT-DNA genes as well as nuclear genes (e.g., complement inhibitors, inflammasome-related genes, lipid transport and epigenetic genes).

Moreover, the H haplogroup cybrids demonstrated decreased cell viability after exposure to amyloid-β_{1-42} peptides (active form) compared to K cybrids. Our data suggest a role for mtDNA-nuclear retrograde signaling in regulation of APOE, a common element in many age-related diseases. Future studies should focus on retrograde signaling from the mitochondria to the nuclear genome that is responsible for these mtDNA-mediated differences.

Acknowledgments

We wish to thank the subjects who participated in this study.

Funding: This work was supported by the Discovery Eye Foundation, Polly and Michael Smith Foundation, Iris and the B. Gerald Cantor Foundation, Beckman Initiative for Macular Research, Max Factor Family Foundation, Lincy Foundation, Guenther Foundation, and the National Institute on Aging [AG006168 to SMJ]. We acknowledge the support of the Institute for Clinical and Translational Science (ICTS) at University of California Irvine.

Abbreviations

5-aza-dC	5-aza-2′-deoxycytidine
AD	Alzheimer's disease
AMD	Age-related Macular Degeneration
APOE	apolipoprotein E
ARPE-19	retinal pigmented epithelium cell line
ATP	adenosine triphosphate
BSA	bovine serum albumin
DMEM	Dulbecco's modified Eagle's medium
DNA	deoxyribonucleic acid
ECAR	extracellular acidification rate
EDTA	ethylenediaminetetracetic acid
ETC	electron transport chain
FCCP	carbonyl cyanide 4-trifluoromethoxy-phenylhydrazone
IHC	immunohistochemistry
LDL	low density lipid
LHON	Leber hereditary optic neuropathy
μM	micromolar
MDP	mitochondrial derived peptide
Mt	mitochondrial

MT-CYB	mitochondria encoded cytochrome B
MT-ND1	mitochondria encoded NADH dehydrogenase 1
MT-ND4	mitochondria encoded NADH dehydrogenase 4
MT-ND5	mitochondria encoded NADH dehydrogenase 5
MT-ND6	mitochondria encoded NADH dehydrogenase 6
MT-CO1	mitochondria encoded cytochrome oxidase 1
MT-CO2	mitochondria encoded cytochrome oxidase 2
MT-CO3	mitochondria encoded cytochrome oxidase 3
MT-ATP6	mitochondria Encoded ATP synthase 6
MT-ATP8	mitochondria Encoded ATP synthase 8
NFkB2	nuclear factor of kappa light polypeptide gene enhancer in B-cells 2
OCR	oxygen consumption rate
OXPHOS	oxidative phosphorylation
Q-PCR	quantitative polymerase chain reaction
PCR	polymerase chain reaction
Rho0	lacking mtDNA
ROS	reactive oxygen species
RPE	retinal pigment epithelial
SEM	standard error mean
SNPs	single nucleotide polymorphisms
$VO2_{max}$	maximal oxygen uptake

References

Arning L, Haghikia A, Taherzadeh-Fard E, et al. Mitochondrial haplogroup H correlates with ATP levels and age at onset in Huntington disease. J Mol Med (Berl). 2010; 88(4):431–436. [PubMed: 20108082]

Atilano SR, Malik D, Chwa M, et al. Mitochondrial DNA variants can mediate methylation status of inflammation, angiogenesis and signaling genes. Hum Mol Genet. 2015; 24(16):4491–4503. [PubMed: 25964427]

Atzmon G, Rincon M, Rabizadeh P, Barzilai N. Biological evidence for inheritance of exceptional longevity. Mech Ageing Dev. 2005; 126(2):341–345. [PubMed: 15621216]

Behar DM, Hammer MF, Garrigan D, et al. MtDNA evidence for a genetic bottleneck in the early history of the Ashkenazi Jewish population. Eur J Hum Genet. 2004; 12(5):355–364. [PubMed: 14722586]

Bellizzi D, Taverna D, D'Aquila P, et al. Mitochondrial DNA variability modulates mRNA and intra-mitochondrial protein levels of HSP60 and HSP75: experimental evidence from cybrid lines. Cell Stress Chaperones. 2009; 14(3):265–271. [PubMed: 18815895]

Bellizzi D, D'Aquila P, Giordano M, et al. Global DNA methylation levels are modulated by mitochondrial DNA variants. Epigenomics. 2012; 4(1):17–27. [PubMed: 22332655]

Bellizzi D, D'Aquila P, Scafone T, et al. The control region of mitochondrial DNA shows an unusual CpG and non-CpG methylation pattern. DNA Res. 2013; 20(6):537–547. [PubMed: 23804556]

Berchuck A, Carney M, Lancaster JM, et al. Familial breast-ovarian cancer syndromes: BRCA1 and BRCA2. Clin Obstet Gynecol. 1998; 41(1):157–166. [PubMed: 9504233]

Bi R, Zhang W, Yu D, et al. Mitochondrial DNA haplogroup B5 confers genetic susceptibility to Alzheimer's disease in Han Chinese. Neurobiol Aging. 2015; 36(3):1604 e7–1604 16.

Bulstrode H, Nicoll JA, Hudson G, et al. Mitochondrial DNA and traumatic brain injury. Ann Neurol. 2014; 75(2):186–195. [PubMed: 24523223]

Canter JA, Kallianpur AR, Fowke JH. Re: North American white mitochondrial haplogroups in prostate and renal cancer. J Urol. 2006; 176(5):2308–2309. (author reply 9).

Canter JA, Olson LM, Spencer K, et al. Mitochondrial DNA polymorphism A4917G is independently associated with age-related macular degeneration. PLoS One. 2008; 3(5):e2091. [PubMed: 18461138]

Carrieri G, Bonafe M, De Luca M, et al. Mitochondrial DNA haplogroups and APOE4 allele are non-independent variables in sporadic Alzheimer's disease. Hum Genet. 2001; 108(3):194–198. [PubMed: 11354629]

Chen A, Raule N, Chomyn A, Attardi G. Decreased reactive oxygen species production in cells with mitochondrial haplogroups associated with longevity. PLoS One. 2012; 7(10):e46473. [PubMed: 23144696]

Czarnecka AM, Bartnik E. The role of the mitochondrial genome in ageing and carcinogenesis. J Aging Res. 2011; 2011:136435. [PubMed: 21403887]

De Luca A, Nasi M, Di Giambenedetto S, et al. Mitochondrial DNA haplogroups and incidence of lipodystrophy in HIV-infected patients on long-term antiretroviral therapy. J Acquir Immune Defic Syndr. 2012; 59(2):113–120. [PubMed: 22245716]

Di Francesco A, Arosio B, Falconi A, et al. Global changes in DNA methylation in Alzheimer's disease peripheral blood mononuclear cells. Brain Behav Immun. 2015; 45:139–144. [PubMed: 25452147]

Dorey E, Chang N, Liu QY, et al. Apolipoprotein E, amyloid-beta, and neuroinflammation in Alzheimer's disease. Neurosci Bull. 2014; 30(2):317–330. [PubMed: 24652457]

Dunn KC, Marmorstein AD, Bonilha VL, et al. Use of the ARPE-19 cell line as a model of RPE polarity: basolateral secretion of FGF5. Invest Ophthalmol Vis Sci. 1998; 39(13):2744–2749. [PubMed: 9856785]

Fernandez-Caggiano M, Barallobre-Barreiro J, Rego-Perez I, et al. Mitochondrial haplogroups H and J: risk and protective factors for ischemic cardiomyopathy. PLoS One. 2012; 7(8):e44128. [PubMed: 22937160]

Fernandez-Caggiano M, Barallobre-Barreiro J, Rego-Perez I, et al. Mitochondrial DNA haplogroup H as a risk factor for idiopathic dilated cardiomyopathy in Spanish population. Mitochondrion. 2013; 13(4):263–268. [PubMed: 23528301]

Fesahat F, Houshmand M, Panahi MS, et al. Do haplogroups H and U act to increase the penetrance of Alzheimer's disease? Cell Mol Neurobiol. 2007; 27(3):329–334. [PubMed: 17186363]

Fetterman JL, Zelickson BR, Johnson LW, et al. Mitochondrial genetic background modulates bioenergetics and susceptibility to acute cardiac volume overload. Biochem J. 2013; 455(2):157–167. [PubMed: 23924350]

Gomez-Duran A, Pacheu-Grau D, Lopez-Gallardo E, et al. Unmasking the causes of multifactorial disorders: OXPHOS differences between mitochondrial haplogroups. Hum Mol Genet. 2010; 19(17):3343–3353. [PubMed: 20566709]

Graham DI, Horsburgh K, Nicoll JA, Teasdale GM. Apolipoprotein E and the response of the brain to injury. Acta Neurochir Suppl. 1999; 73:89–92. [PubMed: 10494348]

Grimaldi V, Vietri MT, Schiano C, et al. Epigenetic reprogramming in atherosclerosis. Curr Atheroscler Rep. 2015; 17(2):476. [PubMed: 25433555]

Guha M, Avadhani NG. Mitochondrial retrograde signaling at the crossroads of tumor bioenergetics, genetics and epigenetics. Mitochondrion. 2013; 13(6):577–591. [PubMed: 24004957]

Guha S, Rosenfeld JA, Malhotra AK, et al. Implications for health and disease in the genetic signature of the Ashkenazi Jewish population. Genome Biol. 2012; 13(1):R2. [PubMed: 22277159]

Hatzfeld JJ, LaVeist TA, Gaston-Johansson FG. Racial/ethnic disparities in the prevalence of selected chronic diseases among US Air Force members, 2008. Prev Chronic Dis. 2012; 9:E112. [PubMed: 22698173]

Hjelmeland LM. Dark matters in AMD genetics: epigenetics and stochasticity. Invest Ophthalmol Vis Sci. 2011; 52(3):1622–1631. [PubMed: 21429863]

Hudson G, Carelli V, Spruijt L, et al. Clinical expression of Leber hereditary optic neuropathy is affected by the mitochondrial DNA-haplogroup background. Am J Hum Genet. 2007; 81(2):228–233. [PubMed: 17668373]

Hyttinen JM, Amadio M, Viiri J, et al. Clearance of misfolded and aggregated proteins by aggrephagy and implications for aggregation diseases. Ageing Res Rev. 2014; 18:16–28. [PubMed: 25062811]

Jenkins T, Nicholls E, Gordon E, et al. Familial hypercholesterolaemia—a common genetic disorder in the Afrikaans population. S Afr Med J. 1980; 57(23):943–947. [PubMed: 7404060]

Jones MM, Manwaring N, Wang JJ, et al. Mitochondrial DNA haplogroups and age-related maculopathy. Arch Ophthalmol. 2007; 125(9):1235–1240. [PubMed: 17846364]

Kaarniranta K, Salminen A, Haapasalo A, et al. Age-related macular degeneration (AMD): Alzheimer's disease in the eye? J Alzheimers Dis. 2011; 24(4):615–631. [PubMed: 21297256]

Kenney MC, Hertzog D, Chak G, et al. Mitochondrial DNA haplogroups confer differences in risk for age-related macular degeneration: a case control study. BMC Med Genet. 2013a; 14(1):4. [PubMed: 23302509]

Kenney MC, Chwa M, Atilano SR, et al. Mitochondrial DNA variants mediate energy production and expression levels for CFH, C3 and EFEMP1 genes: implications for age-related macular degeneration. PLoS One. 2013b; 8(1):e54339. [PubMed: 23365660]

Kenney MC, Chwa M, Atilano SR, et al. Molecular and bioenergetic differences between cells with African versus European inherited mitochondrial DNA haplogroups: implications for population susceptibility to diseases. Biochim Biophys Acta. 2014a; 1842(2):208–219. [PubMed: 24200652]

Kenney MC, Chwa M, Atilano SR, et al. Inherited mitochondrial DNA variants can affect complement, inflammation and apoptosis pathways: insights into mitochondrial-nuclear interactions. Hum Mol Genet. 2014b; 23(13):3537–3551. [PubMed: 24584571]

Kurian AK, Cardarelli KM. Racial and ethnic differences in cardiovascular disease risk factors: a systematic review. Ethn Dis. 2007; 17(1):143–152. [PubMed: 17274224]

Lancaster JM, Carney ME, Futreal PA. BRCA 1 and 2—a genetic link to familial breast and ovarian cancer. Medscape Womens Health. 1997; 2(2):7.

Lee C, Zeng J, Drew BG, et al. The mitochondrial-derived peptide MOTS-c promotes metabolic homeostasis and reduces obesity and insulin resistance. Cell Metab. 2015; 21(3):443–454. [PubMed: 25738459]

Lin TK, Lin HY, Chen SD, et al. The creation of cybrids harboring mitochondrial haplogroups in the Taiwanese population of ethnic Chinese background: an extensive in vitro tool for the study of mitochondrial genomic variations. Oxidative Med Cell Longev. 2012; 2012:824275.

Malik D, Hsu T, Falatoonzadeh P, et al. Human retinal transmitochondrial cybrids with J or H mtDNA haplogroups respond differently to ultraviolet radiation: implications for retinal diseases. PLoS One. 2014; 9(2):e99003. [PubMed: 24919117]

McFarland R, Turnbull DM. Batteries not included: diagnosis and management of mitochondrial disease. J Intern Med. 2009; 265(2):210–228. [PubMed: 19192037]

Mensah GA, Mokdad AH, Ford ES, et al. State of disparities in cardiovascular health in the United States. Circulation. 2005; 111(10):1233–1241. [PubMed: 15769763]

Miceli MV, Jazwinski SM. Nuclear gene expression changes due to mitochondrial dysfunction in ARPE-19 cells: implications for age-related macular degeneration. Invest Ophthalmol Vis Sci. 2005; 46(5):1765–1773. [PubMed: 15851580]

Mueller EE, Schaier E, Brunner SM, et al. Mitochondrial haplogroups and control region polymorphisms in age-related macular degeneration: a case–control study. PLoS One. 2012a; 7(2):e30874. [PubMed: 22348027]

Mueller EE, Brunner SM, Mayr JA, et al. Functional differences between mitochondrial haplogroup T and haplogroup H in HEK293 cybrid cells. PLoS One. 2012b; 7(12):e52367. [PubMed: 23300652]

Murrell JR, Price B, Lane KA, et al. Association of apolipoprotein E genotype and Alzheimer disease in African Americans. Arch Neurol. 2006; 63(3):431–434. [PubMed: 16533971]

Naviaux RK. Mitochondrial control of epigenetics. Cancer Biol Ther. 2008; 7(8):1191–1193. [PubMed: 18719362]

Pacheu-Grau D, Gomez-Duran A, Iglesias E, et al. Mitochondrial antibiograms in personalized medicine. Hum Mol Genet. 2013; 22(6):1132–1139. [PubMed: 23223015]

Pogribny IP, Rusyn I. Environmental toxicants, epigenetics, and cancer. Adv Exp Med Biol. 2013; 754:215–232. [PubMed: 22956504]

Ratnayaka JA, Serpell LC, Lotery AJ. Dementia of the eye: the role of amyloid beta in retinal degeneration. Eye (Lond). 2015; 29(8):1013–1026. [PubMed: 26088679]

Ridge PG, Maxwell TJ, Corcoran CD, et al. Mitochondrial genomic analysis of late onset Alzheimer's disease reveals protective haplogroups H6A1A/H6A1B: the Cache County Study on memory in aging. PLoS One. 2012; 7(9):e45134. [PubMed: 23028804]

Romero JR, Preis SR, Beiser A, et al. Risk factors, stroke prevention treatments, and prevalence of cerebral microbleeds in the Framingham Heart Study. Stroke. 2014; 45(5):1492–1494. [PubMed: 24713533]

Salminen A, Haapasalo A, Kauppinen A, et al. Impaired mitochondrial energy metabolism in Alzheimer's disease: impact on pathogenesis via disturbed epigenetic regulation of chromatin landscape. Prog Neurobiol. 2015; 131:1–20. [PubMed: 26001589]

SanGiovanni JP, Arking DE, Iyengar SK, et al. Mitochondrial DNA variants of respiratory complex I that uniquely characterize haplogroup T2 are associated with increased risk of age-related macular degeneration. PLoS One. 2009; 4(5):e5508. [PubMed: 19434233]

Seftel HC, Baker SG, Jenkins T, Mendelsohn D. Prevalence of familial hypercho-lesterolemia in Johannesburg Jews. Am J Med Genet. 1989; 34(4):545–547. [PubMed: 2624266]

Smiraglia DJ, Kulawiec M, Bistulfi GL, et al. A novel role for mitochondria in regulating epigenetic modification in the nucleus. Cancer Biol Ther. 2008; 7(8):1182–1190. [PubMed: 18458531]

Strauss KA, DuBiner L, Simon M, et al. Severity of cardiomyopathy associated with adenine nucleotide translocator-1 deficiency correlates with mtDNA haplogroup. Proc Natl Acad Sci U S A. 2013; 110(9):3453–3458. [PubMed: 23401503]

Sun E, Lim A, Liu X, et al. Apolipoprotein E gene and age-related macular degeneration in a Chinese population. Mol Vis. 2011; 17:997–1002. [PubMed: 21541275]

Udar N, Atilano SR, Memarzadeh M, et al. Mitochondrial DNA haplogroups associated with age-related macular degeneration. Invest Ophthalmol Vis Sci. 2009; 50(6):2966–2974. [PubMed: 19151382]

Verghese PB, Castellano JM, Garai K, et al. ApoE influences amyloid-beta (Abeta) clearance despite minimal apoE/Abeta association in physiological conditions. Proc Natl Acad Sci U S A. 2013; 110(19):E1807–E1816. [PubMed: 23620513]

Wallace DC. Diseases of the mitochondrial DNA. Annu Rev Biochem. 1992; 61:1175–1212. [PubMed: 1497308]

Wallace DC. Mitochondrial DNA mutations in diseases of energy metabolism. J Bioenerg Biomembr. 1994; 26(3):241–250. [PubMed: 8077179]

Wallace DC, Fan W. Energetics, epigenetics, mitochondrial genetics. Mitochondrion. 2010; 10(1):12–31. [PubMed: 19796712]

Wallace, DC., Lott, MT., Procaccio, V. Mitochondrial Genes in Degenerative Diseases, Cancer and Aging. fifth. Vol. 1. Churchill Livingstone Elsevier; Philadelphia, PA: 2007. p. 194-298.(Chapter 13)

Whelan SP, Zuckerbraun BS. Mitochondrial signaling: forwards, backwards, and in between. Oxidative Med Cell Longev. 2013; 2013:351613.

Yen K, Lee C, Mehta H, Cohen P. The emerging role of the mitochondrial-derived peptide humanin in stress resistance. J Mol Endocrinol. 2013; 50(1):R11–R19. [PubMed: 23239898]

Zaragoza MV, Brandon MC, Diegoli M, et al. Mitochondrial cardiomyopathies: how to identify candidate pathogenic mutations by mitochondrial DNA sequencing, MITOMASTER and phylogeny. Eur J Hum Genet. 2011; 19(2):200–207. [PubMed: 20978534]

Zhang F, Pracheil T, Thornton J, Liu Z. Adenosine triphosphate (ATP) is a candidate signaling molecule in the mitochondria-to-nucleus retrograde response pathway. Genes (Basel). 2013; 4(1): 86–100. [PubMed: 24605246]

Zhao Y, Bhattacharjee S, Jones BM, et al. Beta-amyloid precursor protein (betaAPP) processing in Alzheimer's disease (AD) and age-related macular degeneration (AMD). Mol Neurobiol. 2015; 52(1):533–544. [PubMed: 25204496]

a

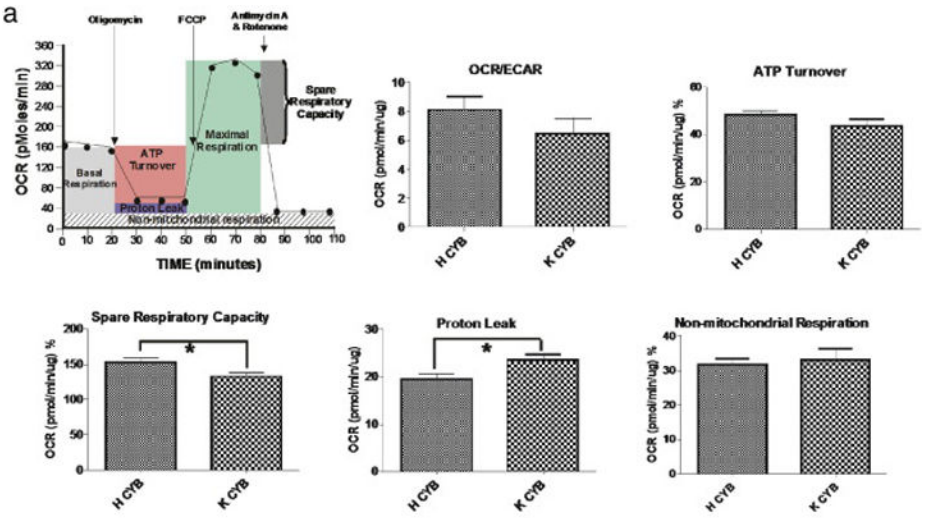

b

Symbol	Gene Name	H vs. K $\Delta\Delta C_T$ / Fold	H vs. K p-value
MT-ND1	NADH Dehydrogenase subunit 1	1.07±0.27 / 2.10	**0.0011**
MT-ND2	NADH Dehydrogenase subunit 2	0.63±0.37 / 1.55	0.1073
MT-ND3	NADH Dehydrogenase subunit 3	0.59±0.41 / 1.51	0.1762
MT-ND4/ND4L	NADH Dehydrogenase subunit 4/4L	0.70±0.23 / 1.62	**0.0078**
MT-ND5	NADH Dehydrogenase subunit 5	1.61±0.12 / 3.05	**<0.0001**
MT-ND6	NADH Dehydrogenase subunit 6	1.31±0.18 / 2.48	**<0.0001**
MT-CO1	Cytochrome c oxidase subunit I	1.78±0.19 / 3.43	**<0.0001**
MT-CO2	Cytochrome c oxidase subunit II	1.14±0.22 / 2.2	**<0.0001**
MT-CO3	Cytochrome c oxidase subunit III	1.07±0.21 / 2.10	**0.0001**
MT-CYB	Cytochrome b	1.15±0.24 / 2.22	**0.0002**
MT-ATP6	ATP synthase F0 subunit 6	1.03±0.24 / 2.04	**0.0005**
MT-ATP8	ATP synthase F0 subunit 8	1.20±0.22 / 2.30	**<0.0001**

Positive values indicate up regulation of the gene. Negative values indicate down regulation of the gene. H cybrids are assigned a value of 1. Fold = $2^{-\Delta\Delta CT}$

c

	Day 1	Day 7
H Cybrids	1.44 ± 0.014	1.33 ± 0.031
K Cybrids	1.29 ± 0.014 ($p < 0.0001$)	1.19 ± 0.033 ($p < 0.0055$)

Fig. 1.

(1a) Schematic representation of oxygen consumption rate (OCR); showing basal aerobic respiration, ATP turnover, maximal respiration, spare respiratory capacity, proton leak and non-mitochondrial respiration measured by Seahorse XF24 flux analyzer. No differences were found between H and K cybrids for the OCR/ECAR ratio ($p > 0.27$); ATP turnover after oligomycin treatment ($p > 0.24$) or non-mitochondrial respiration ($p > 0.73$). In response to antimycin A plus rotenone, the K cybrids showed significantly decreased spare respiratory capacity ($p < 0.014$) and increased in proton leak in K cybrids relative to the H

cybrids ($p < 0.022$). Haplo, haplogroup. (1b) Table shows the different levels of expression for mtDNA-encoded genes in the H cybrids compared to K cybrids. Although all cybrids have identical nuclei, the K cybrids have upregulation of ten genes compared to the H cybrids. (1c) The K cybrids had significantly lower mtDNA copy numbers compared to H cybrids at Day 1 and Day 7 incubation period. The mtDNA copy number was determined by measuring the ratio of nuclear DNA (18S) and mtDNA (MT-ND2).

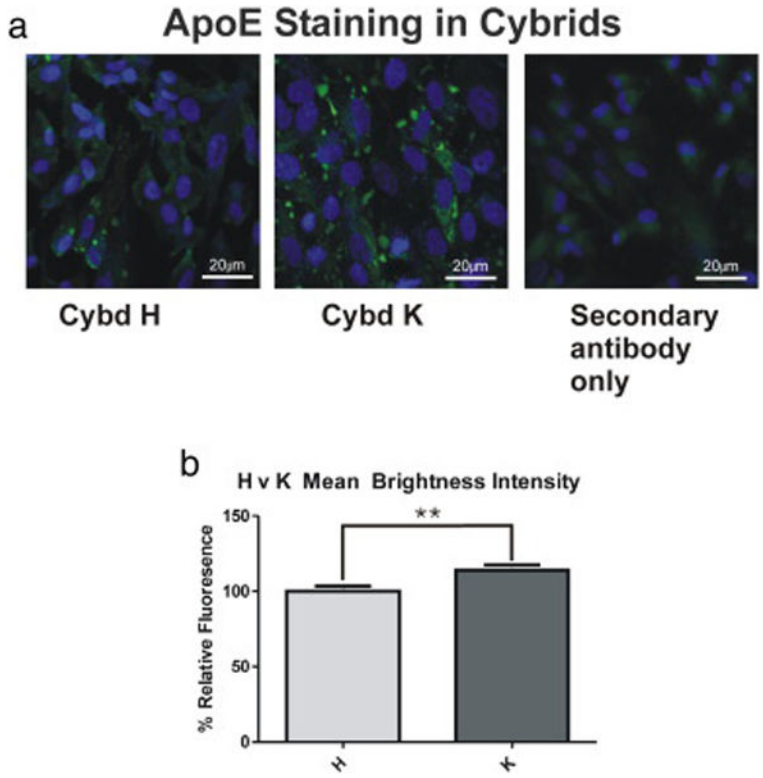

Fig. 2.

Immunohistochemistry studies show K cybrids had increased ApoE staining compared to H cybrids. H (n = 6) and K (n = 7) cybrid cell cultures were stained with polyclonal ApoE antibody and nuclei were visualized by staining with DAPI (blue). Cells were examined and photographed with fluorescent microscopy. Representative staining are shown for H cybrids and K cybrids. The H cybrids showed a punctate, peripheral staining while K cybrids showed larger, more globular staining. Secondary antibody staining was negative. Scale bars represent 20 μm. Cybd, cybrid.

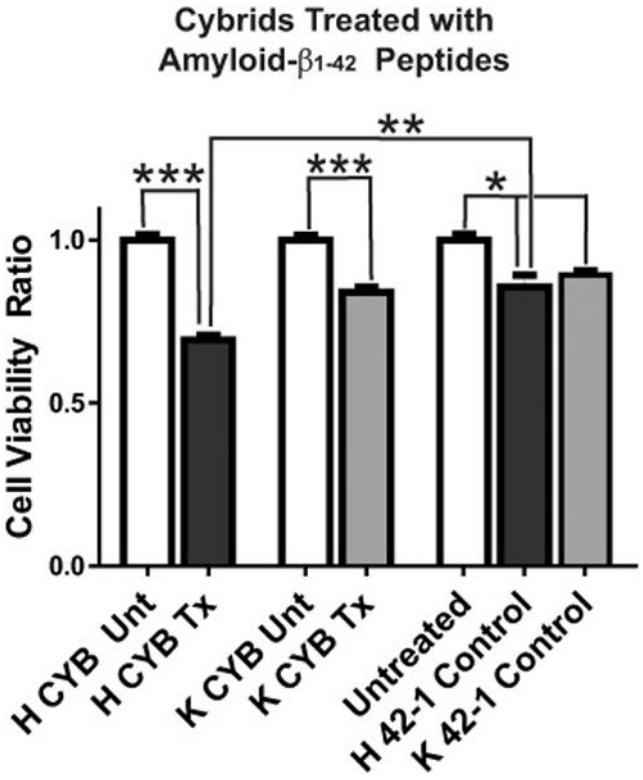

Fig. 3.

The H cybrids were more sensitive to amyloid-$\beta_{1–42}$ toxicity compare to the K cybrids. H and K cybrids were treated 24 h with amyloid-$\beta_{1–42}$ peptide (active form) or the amyloid-$\beta_{42–1}$ peptide (inactive form) and cell viability was measured. All values shown are percent relative to untreated (100% value). The cell viability for amyloid-$\beta_{1–42}$ treated H cybrids was 70% ± 2.3% viable ($p < 0.0001$). The viability for amyloid-$\beta_{1–42}$ treated K cybrids was 84% ± 2.0% ($p < 0.0001$). The inactive amyloid-$\beta_{42–1}$ peptide control was 90% ± 1.5% viable ($p = 0.01$). Cybd, Cybrid; Unt, Untreated; Tx, Treated.

a

Symbol	Gene Name	GenBank Accession No.	Function	H vs. K p-value	H vs. K $\Delta\Delta C_T$ / Fold
HAT1	Histone acetyltransferase	NM_001033085 NM_003642	Adds acetyl group; promotes transcription.	0.04	-0.4 ± 0.2/ 0.8-fold
HDAC1	Histone deacetylase 1	NM_004964	Class I histone deacetylase involved in control of cell proliferation, differentiation, growth and apoptosis; Represses transcription.	0.6	0.06 ± 0.13/ 1.1-fold
HDAC6	Histone deacetylase 6	NM_006044	Class II histone deacetylase.	0.06	-0.4 ± 0.2/ 0.7-fold
HDAC11	Histone deacetylase 11	NM_024827	Class IV histone deacetylase localized to the nucleus; Involved in regulating interleukin 10 expression.	0.4	-0.2 ± 0.2/ 0.9-fold
SIN3A	Sin3 transcription regulator homolog A (yeast)	NM_001145357 NM_001145358 NM_015477	Transcriptional regulator for STAT3; Promotes deacetylation.	0.0006	-0.5 ± 0.1/ 0.7-fold
MAT2B	Methionine adenosyltransferase II, beta	NM_013283	Catalyzes the biosynthesis of S-adenosylmethionine, the major methyl donor; Regulatory beta subunit.	0.9	0.02 ± 0.1/ 1.0-fold
MBD2	methyl-CpG binding domain protein 2	NM_003927	Part of nuclear protein family related by the presence of a methyl-CpG binding domain (MBD). Binds specifically to methylated DNA; represses transcription from methylated gene promoters; functions as a demethylase to activate transcription.	0.16	-0.3 ± 0.2/ 0.8-fold
MBD4	Methyl-CpG binding domain protein 4	NM_003925	Binds specifically to methylated DNA; Involved in protein interactions, & DNA repair.	<0.0001	-0.9 ± 0.2/ 0.5-fold
DNMT1	DNA (cystosine-5) methyltransferase 1	NM_001130823 NM_001379	Methylates CpG residues, preferentially methylates hemimethylated DNA. Associates with DNA replication sites in S phase	<0.0001	-0.8 ± 0.2/ 0.6-fold
			maintaining the methylation pattern in newly synthesized strand, essential for epigenetic inheritance.		
DNMT3A	DNA (cystosine-5) methyltransferase 3A	NM_022552 NM_153759 NM_175629	Methylates de novo during development. Important for genomic imprinting.	0.03	0.5 ± 0.2/ 1.4-fold
DNMT3B	DNA (cystosine-5) methyltransferase 3B	NM_001207055 NM_001207056 NM_006892 NM_175848 NM_175849 NM_175850	Methylates de novo during development. Important for genomic imprinting.	0.002	-0.7 ± 0.2/ 0.6-fold

Positive values indicate up regulation of the gene. Negative values indicate down regulation of the gene.
The values for the H cybrids are equal to 1. Fold = $2^{\Delta\Delta CT}$;
N = 6 to 8 biologically different cybrids in the H and K groups were evaluated with three replicate values for each sample.

b

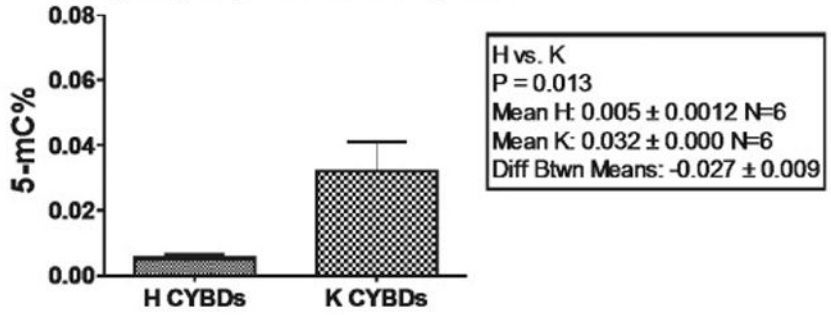

c

Symbol	H Cybrids vs K Cybrids (Untreated) p-value $\Delta\Delta C_T$ / Fold	H Cybrids vs K Cybrids (5-aza-dC Treated) p-value $\Delta\Delta C_T$ / Fold
*APOE**	0.001 1.21 ± 0.34 / 2.3	<0.0001 2 ± 0.31 / 3.8
*NFκB2**	0.004 1.56 ± 0.47 / 3	0.07 0.53 ± 0.27 / 1.5

Value greater than 1 indicates upregulation of the gene.
Value less than 1 indicates downregulation of the gene.
K cybrids, n = 3 different individuals; H cybrids, n = 3 different individuals.
The H cybrid were assigned a value of 1.
Each sample was run in triplicate and experiment was repeated twice
Fold = $2^{-\Delta\Delta CT}$
*versus housekeeper HMBS.

Fig. 4.

(4a) Shows differential RNA expression of epigenetic genes in the H cybrids ($n = 6$) compared to the K cybrid ($n = 6$). Q-PCR analyses were performed and the H cybrid values were equal to 1. Fold differences were calculated using $2^{\Delta\Delta CT}$. The gene symbols, full name, GenBank No., and brief description of function are described. (4b) The K cybrids ($n = 6$) had a 6.2-fold higher global methylation level compare to the H cybrids ($n = 6$) ($p = 0.013$). (4c) Expression levels of *APOE* and *NFκB2* before and after treatment with 5-aza-dC, a methylation inhibitor are shown. The *APOE* transcription levels were significantly higher in the K cybrids for both the untreated and 5-aza-dC treated cultures compared to the H cybrids, indicating differences in expression levels are not due to methylation status of the cells. In contrast, the untreated K cybrids had a higher levels of *NFκB2* compared to the H cybrids, but after 5-aza-dC treatment the *NFκB2* expression levels were similar. CYBD, Cybrid.

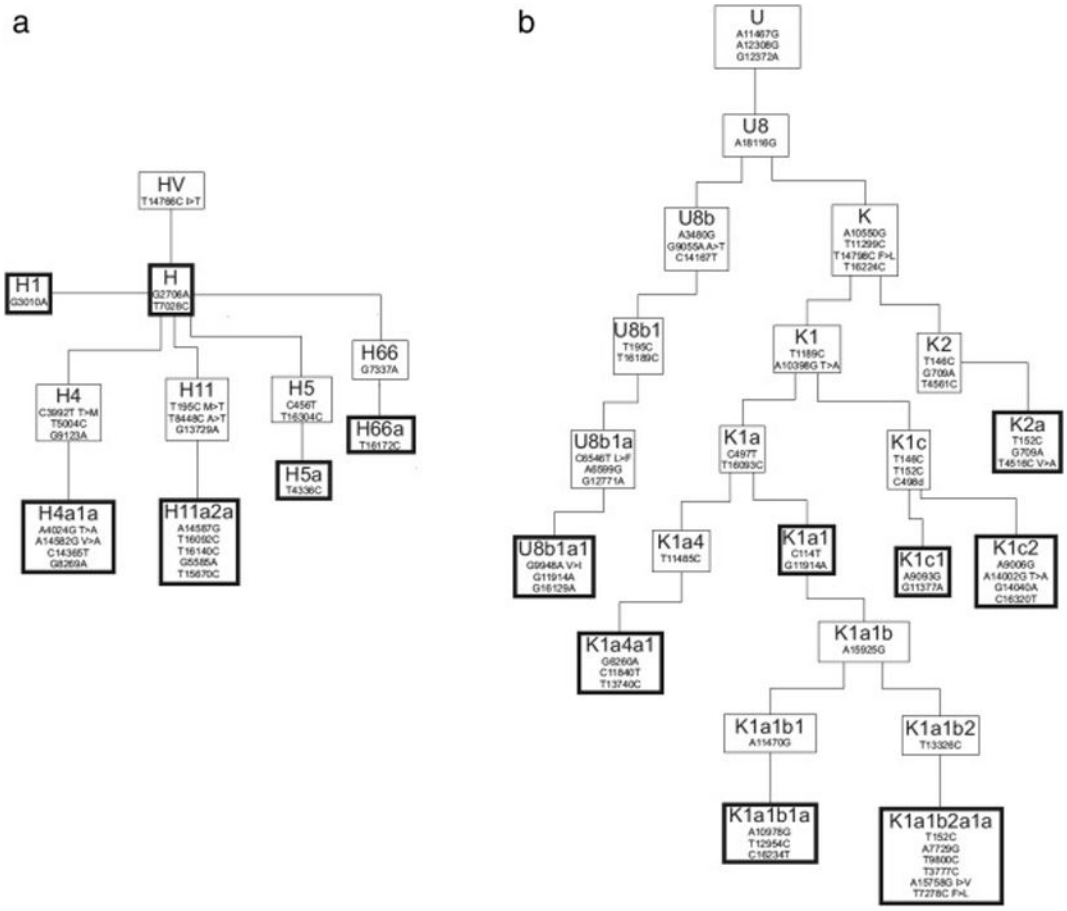

Fig. 5.

a and b Flow chart showing the K haplogroup and H haplogroup subsets of individuals used to create cybrids (bolded boxes). The amino acid changes are listed next to the non-synonymous SNPs.

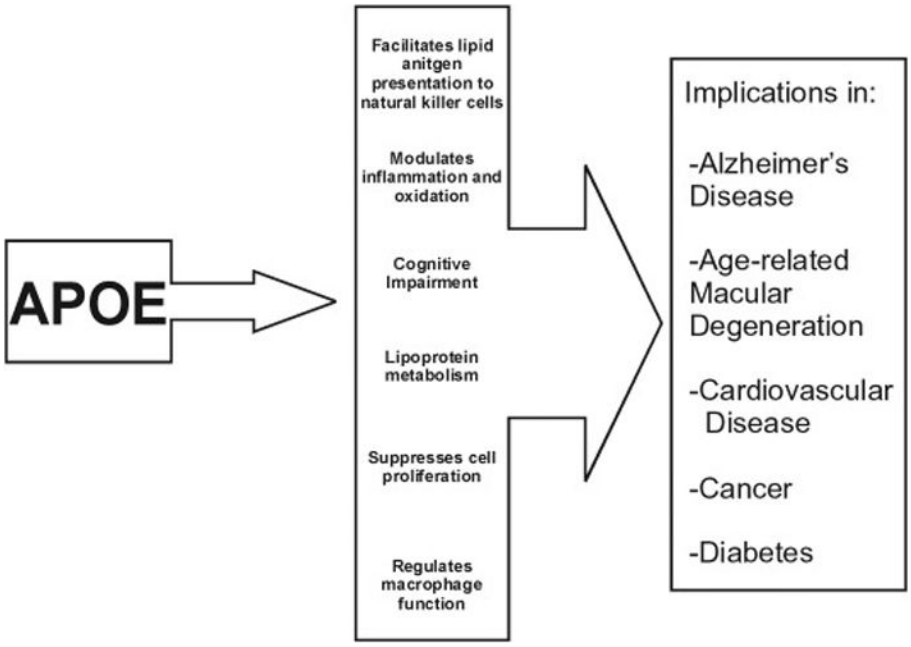

Fig. 6.

Schematic figure shows that ApoE has been linked to systemic physiological impairments, which have underlying implications in a variety of diseases.

Table 1

Background information for cybrid samples.

Cybrid no.	Gender	Age	Haplogroup
10-03	M	24	H
10-04	M	33	H5a
10-07	M	49	H66a
11-10	M	30	H4a1a
11-23	F	22	H11a2a2
11-35	F	30	H1
13-45	F	45	H
13-49	M	26	H1
13-52	F	58	H1
13-56	F	21	H
13-65	F	52	H4a1a
11-08	M	24	K1c1
11-25	M	22	K2a
11-34	M	66	U8b1a1
13-47	F	38	K1a4a1
13-57	F	45	K1a1
13-64	F	38	K1a1b1a
13-75	F	56	K1c2
13-77	F	57	K1a1b1a
13-80	F	46	K1a1b2a1a
13-103	F	25	K

Table 2

Genes found in atherosclerotic pathways as identified by human genome U133 plus 2.0 array and analyzed with the networks system ingenuity program.

		Genes found in atherosclerosis signaling pathways				
Probe set ID	**Representative public ID**	**gene title**	**Gene symbol**	**K cybrids mas5-signal**	**CY H cybrids 20111222. mas5-signal**	**Fold differences in K vs H cybrids**
203381_s_at	N33009	Apolipoprotein E	APOE	840.68	135.81	6.19
203382_s_at	NM_000041	Apolipoprotein E	APOE	770.93	187.10	4.12
212884_x_at	AI358867	Apolipoprotein E	APOE	569.31	376.69	1.51
212883_at	AI358867	Apolipoprotein E	APOE	22.03	18.57	1.19
212874_at	AI358867	Apolipoprotein E	APOE	2.59	6.44	−2.48
204416_x_at	NM_001645	Apolipoprotein C-I	APOC1	99.30	34.38	2.89
213553_x_at	W79394	Apolipoprotein C-I	APOC1	40.01	196.2	−4.9
217430_x_at	Y15916	Collagen, type I, alpha 1	COL1A1	337.20	226.35	1.49
202312_s_at	NM_000088	Collagen, type I, alpha 1	COL1A1	63.20	61.28	1.03
202310_s_at	K01228	Collagen, type I, alpha 1	COL1A1	53.87	191.70	−3.56
202311_s_at	AI743621	Collagen, type I, alpha 1	COL1A1	9.19	38.54	−4.19
1556499_s_at	BE221212	Collagen, type I, alpha 1	COL1A1	76.35	847.33	−11.10
204475_at	NM_002421	Matrix metallopeptidase 1 (interstitial collagenase)	MMP1	562.03	118.67	4.74

Table 3

Q-PCR shows differential gene expression patterns for H cybrids versus the K cybrids for genes in various pathways.

			Atherosclerosis & lipid transport		
Symbol	**Gene name**	**GenBank accession No.**	**Functions**	**H vs. K *p*-value**	**H vs. K $\Delta\Delta C_T$/fold**
APOE	Apolipoprotein, E	NM_000041	Main apoprotein of chylomicron that binds to a specific receptor on liver cells and peripheral cells. ApoE is essential for the normal catabolism of triglyceride-rich lipoprotein constituents.	<0.0001	3.21 ± 0.41/9.3
APOC1	Apolipoprotein *C*-I	NM_001645, XM_005258855	The protein encoded by this gene is a member of the apolipoprotein *C*1 family. This gene is expressed primarily in the liver, and it is activated when monocytes differentiate into macrophages. A pseudogene of this gene is located 4 kb downstream in the same orientation, on the same chromosome. This gene is mapped to chromosome 19, where it resides within a apolipoprotein gene cluster. Alternatively spliced transcript variants have been found for this gene, but the biological validity of some variants has not been determined. Inhibits the clearance of lipoprotein particles via VLDLR	0.4	0.21 ± 0.26/1.2
COL1A1	Collagen, type I, alpha 1	NM_000088, XM_005257058, XM_005257059, XM_006721703	This gene encodes the pro-alpha1 chains of type I collagen whose triple helix comprises two alpha1 chains and one alpha2 chain. Type I is a fibril-forming collagen found in most connective tissues and is abundant in bone, cornea, dermis and tendon. Mutations in this gene are associated with osteogenesis imperfecta types I-IV, Ehlers-Danlos syndrome type VIIA, Ehlers-Danlos syndrome Classical type, Caffey Disease and idiopathic osteoporosis. Reciprocal translocations between chromosomes 17 and 22, where this gene and the gene for platelet-derived growth factor beta are located, are associated with a particular type of skin tumor called dermatofibrosarcoma protuberans, resulting from unregulated expression of the growth factor. Two transcripts, resulting from the use of alternate polyadenylation signals, have been identified for this gene.	0.8	0.12 ± 0.42/1.1
MMP1	Matrix metallopeptidase 1	NM_001145938, NM_002421	Proteins of the matrix metalloproteinase (MMP) family are involved in the breakdown of extracellular matrix in normal physiological processes, such as embryonic development, reproduction, and tissue remodeling, as well as in disease processes, such as arthritis and metastasis. Most MMP's are secreted as inactive proproteins which are activated when cleaved by extracellular proteinases. This gene encodes a secreted enzyme which breaks down the interstitial collagens, types I, II, and III. The gene is part of a cluster of MMP genes which localize to chromosome 11q22.3. Alternative splicing results in multiple transcript variants.	0.7	0.03 ± 0.731.2

Symbol	Gene name	GenBank accession No.	Atherosclerosis & lipid transport Functions	H vs. K *p*-value	H vs. K $\Delta\Delta C_T$/fold
			Amyloid beta precursors		
Symbol	Gene NAME	GenBank accession no.	Functions	H vs. K *p*-value	H vs. K $\Delta\Delta C_T$/fold
APBB1IP	Amyloid beta (A4) precursor protein-binding, family B, member 1 interacting protein	NM_019043 XM_006717451	Suppresses transcription factor AP1 activation and SRE sites. Important binding partner for amyloid beta precursor. APBB1 is a member of the Fe65 protein family which is important in Alzheimer's pathology.	*P* = 0.61	−0.25 ± 0.48 0.84
APBB2	Amyloid beta (A4) precursor protein-binding, family B, member 2	NM_001166050 NM_004307 NM_173075 XM_005248101 XM_006714005 XM_006714006 XM_006714007 XM_006714010 XM_006714011 XM_006714012	The protein encoded by this gene interacts with the cytoplasmic domains of amyloid beta (A4) precursor protein and amyloid beta (A4) precursor-like protein 2. This protein contains two phosphotyrosine binding (PTB) domains, which are thought to function in signal transduction. Polymorphisms in this gene have been associated with Alzheimer's disease. Alternative splicing results in multiple transcript variants.	*P* = 0.33	0.20 ± 0.20 1.15
APBA1	Amyloid beta (A4) precursor protein-binding, family A, member 1	NM_001163 XM_005251967 XM_005251968 XM_006717093	The protein encoded by this gene is a member of the ×11 protein family. It is a neuronal adapter protein that interacts with the Alzheimer's disease amyloid precursor protein (APP). It stabilizes APP and inhibits production of proteolytic APP fragments including the A beta peptide that is deposited in the brains of Alzheimer's disease patients. This gene product is believed to be involved in signal transduction processes. It is also regarded as a putative vesicular trafficking protein in the brain that can form a complex with the potential to couple synaptic vesicle exocytosis to neuronal cell adhesion.	*P* = 0.69	0.17 ± 0.43 1.13
			Inflammasome & complement		
Symbol	Gene name	GenBank accession no.	Functions	H vs. K *p*-value	H vs. K $\Delta\Delta C_T$/fold
IL1B	Interleukin 1, beta	NM_000576	Member of the interleukin 1 cytokine family produced by activated macrophages as a proprotein, which is proteolytically processed to its active form by caspase 1. An important mediator of the inflammatory response, and is involved in cell proliferation, differentiation, and apoptosis.	0.001	2.02 ± 0.57/4.1
IL18	Interleukin 18 (interferon-gamma-inducing factor)	NM_001243211 NM_001562	A proinflammatory cytokine that augments natural killer cell activity in spleen cells, and stimulates interferon gamma production in *T*-helper type I cells.	0.0007	1.37 ± 0.37/2.6
CASP1	Caspase 1, apoptosis-related cysteine peptidase	NM_001223 NM_033292 NM_033293 NM_001257118 NM_001257119	This gene encodes a protein which is a member of the cysteine-aspartic acid protease (caspase) family. Sequential activation of caspases plays a central role in the execution-phase of cell apoptosis. Caspases exist as inactive proenzymes which undergo proteolytic processing at	$p < 0.0001$	1.3 ± 0.29/2.5

Symbol	Gene name	GenBank accession No.	Atherosclerosis & lipid transport Functions	H vs. K *p*-value	H vs. K $\Delta\Delta C_T$/fold
			conserved aspartic residues to produce 2 subunits, large and small, that dimerize to form the active enzyme. This gene was identified by its ability to proteolytically cleave and activate the inactive precursor of interleukin-1, a cytokine involved in the processes such as inflammation, septic shock, and wound healing. This gene has been shown to induce cell apoptosis and may function in various developmental stages. Studies of a similar gene in mouse suggest a role in the pathogenesis of Huntington disease. Alternative splicing results in transcript variants encoding distinct isoforms.		
C3	Complement component 3	NM_000064	Central in activation of complement system; required for both classical and alternative pathways.	<0.0001	2.2 ± 0.4/4.4
CFH	Complement factor H	NM_000186	Essential in regulation of complement activation.	0.0012	1.28 ± 0.36/2.4
CD59	CD59 molecule, complement regulatory protein	NM_000611 NM_203329 NM_203331 NM_001127223 NM_001127225 NM_001127226 NM_001127227	Cell surface glycoprotein that regulates complement-mediated cell lysis, inhibits complement membrane attack complex and is involved in lymphocyte signal transduction.	0.004	0.98 ± 0.25/2.0
CD55/DAF	Decay accelerating factor for complement	NM_000574 NM_001114543 NM_001114544 NM_00111475	Involved in regulation of complement cascade by accelerating decay of complement proteins and disrupting the cascade.	0.49	−0.23 ± 0.32/0.9
CFHR4	Complement factor H-related 4	NM_006684 NM_001201550 NM_001201551	One of the 5 CFH-related proteins which enhance the cofactor activity of CFH in C3b inactivation. It can associate with lipoproteins.	0.014	−1.48 ± 0.49/0.4
CFP	Complement factor properdin	NM_001145252NM_002621	Plasma glycoprotein that positively regulates the alternative complement pathway. Binds many microbial surfaces and apoptotic cells and stabilizes C3 and C5 convertases to lead to the formation of the membrane attack complex and lysis of target cells.	0.078	0.49 ± 0.26/0.7
C4B	Complement component 4B (Chido blood group)	NM_001002029 NM_000592	Basic form of complement factor 4, classical pathway. Provides surface for interaction between antigen-antibody complex and complement components.	0.24	0.87 ± 0.71/1.8
C1S	Complement component 1, s subcomponent	NM_001734 NM_201442	A serine protease, which is the major constituent of complement subcomponent 1. C1s associates with C1r and C1q to yield the first component of the serum complement system.	0.51	−2.28 ± 1.14/0.2
C1QC	Complement component 1, q subcomponent, C chain	NM_001114101 NM_172369	Major constituent of complement subcomponent, C1q which associates with C1r and C1s to yield the first component of the serum complement system.	0.12	−0.69 ± 0.24/0.62
CFD	Complement factor D	NM_001928	Serine protease that cleaves factor B bound to C3b to yield C3bBb. Factor D is the initial obligatory and rate-limiting	0.009	0.83 ± 0.3/1.8

Symbol	Gene name	GenBank accession No.	Atherosclerosis & lipid transport Functions	H vs. K *p*-value	H vs. K $\Delta\Delta C_T$/fold
			catalytic component in the alternative complement pathway.		
CFI	Complement factor I	NM_000204	Plasma glycoprotein, serine proteinase cleaves and inactivates C4b and C3b activities.	0.025	1.15 ± 0.49/2.2
IL-6	Interleukin 6	NM_000600	Cytokine involved in inflammation and maturation of B cells.	0.31	−1.23 ± 1.16/0.4
IL-33	Interleukin 33	NM_033439 NM_001199640 NM_001127180	Member of IL1 family; critical pro-inflammatory cytokine involved in production of T helper-2-associated cytokines.	0.4	0.43 ± 0.52/1.4
TGFA	Transforming growth factor, alpha	NM_003236 NM_001099691	Ligand for EGFR which activates signaling pathway for cell proliferation, differentiation, and development	0.07	−1.10 ± 0.57/0.47
TGFB2	Transforming growth factor, beta 2	NM_003238 NM_001135599	Secreted cytokine that regulates proliferation, differentiation, adhesion, migration and other functions.	0.23	−0.80 ± 0.63/0.57
			Signaling pathways		
Symbol	Gene name	GenBank accession no.	Functions	H vs. K *p*-value	H vs. K $\Delta\Delta C_T$/fold
THBS1	Thrombospondin 1	NM_003246	Subunit of a disulfide-linked homotrimeric protein that is an adhesive glycoprotein that mediates cell-to-cell and cell-to-matrix interactions. Can bind to fibrinogen, fibronectin, laminin, type V collagen and integrins alpha-V/beta-1 and involved in platelet aggregation, angiogenesis, and tumorigenesis.	0.0009	−1.3 ± 0.35/0.4
HSPG2	Heparan sulfate proteoglycan 2	NM_005529	Encodes perlecan protein that binds to and crosslinks extracellular matrix and cell-surface molecules.	0.3	−0.25 ± 0.2/0.8-fold
ITGB5	Integrin, beta 5	NM_002213	Mediates cell-cell and cell-extracellular matrix interactions	0.2	−0.35 ± 0.27/0.8
ITGB8*	Integrin, beta 8	NM_002214	Encodes a single-pass type I membrane protein; mediates cell-cell and cell-extracellular matrix interactions and involved in airway epithelial proliferation	<0.0001	1.1 ± 0.13/1.5
NFKβ2	Nuclear factor of kappa light polypeptide gene enhancer in B-cells 2	NM_001077494 NM_001077493 NM_002502	Subunit of transcription factor complex nuclear factor-kappa-B complex which is central activator of inflammation and immune function genes.	0.005	0.6 ± 0.2/1.5
MAPK8	Mitogen-activated protein kinase 8	NM_139046 NM_002750 NM_139047 NM_139049	Targets specific transcription factors, mediates immediate-early gene expression, involved in UV radiation induced apoptosis.	0.29	0.18 ± 0.16/1.1
MAPK10	Mitogen-activated protein kinase 10	NM_002753 NM_138980 NM_138982	Regulatory role in signaling pathways during neuronal apoptosis, inhibited by cyclin dependent kinase 5.	0.71	−0.2 ± 0.52/0.9
			Housekeeper genes		

			Atherosclerosis & lipid transport		
Symbol	**Gene name**	**GenBank accession No.**	**Functions**	**H vs. K *p*-value**	**H vs. K $\Delta\Delta C_T$/fold**
HPRT1	Hypoxanthine phosphoribosyl-transferase 1	NM_000194	Transferase which catalyzes conversion of hypoxanthine to inosine monophosphate & guanine to guanosine monophosphate. Plays a central role in the generation of purine nucleotides through the purine salvage pathway. Endogenous control.		
HMBS	Hydroxymethyl-bilane synthase	NM_000190 NM_001024382 NM_001258208 NM_001258209	Member of the hydroxymethylbilane synthase superfamily. Third enzyme of the heme biosynthetic pathway. Catalyzes the head to tail condensation of four porphobilinogen molecules into the linear hydroxymethylbilane. Endogenous control.		
ALASv1	5′-aminolevulinate synthase 1	NM_000688 XM_005264944	This gene encodes the mitochondrial enzyme which catalyzes the rate-limiting step in heme (iron-protoporphyrin) biosynthesis. The enzyme encoded by this gene is the housekeeping enzyme; The level of the mature encoded protein is regulated by heme: high levels of heme down-regulate the mature enzyme in mitochondria while low heme levels up-regulate.		
TUBB	Tubulin beta class I	NM_178014, NM_001293213	Belongs to a protein superfamily of globular proteins and is the major component of microtubules.		
GUSB	Glucuronidase, beta	NM_000181 NM_001284290 NM_001293104 NM_001293105 XM_005250297	Belongs to the glycosidase family of enzymes that break down complex carbohydrates.		

Positive values indicate up regulation of the gene. Negative values indicate down regulation of the gene.

The values for the H cybrids are equal to 1. Fold = $2^{\Delta\Delta CT}$;

There were $N = 6–8$ biologically different cybrids in the H and K groups, with three replicate values for each sample.